JOURNAL OF AGRICULTURAL AND FOOD CHEMISTRY

ARTICLE

pubs.acs.org/JAFC

Cloning of a Novel L-Amino Acid Oxidase from *Trichoderma harzianum* ETS 323 and Bioactivity Analysis of Overexpressed L-Amino Acid Oxidase

Chi-Hua Cheng,[†] Chia-Ann Yang,[‡] Shu-Ying Liu,[§] Chaur-Tsuen Lo,[∥] Hsiou-Chen Huang,[⊥] Fang-Chin Liao,[∥,⊥] and Kou-Cheng Peng*[,†]

[†]Institute of Biotechnology, National Dong Hwa University, Hualien 97401, Taiwan, Republic of China

[‡]Institute of Medical Science, Tzu Chi University, Hualien 97004, Taiwan, Republic of China

[§]Department of Molecular Biotechnology, Da-Yeh University, Changhua 51591, Taiwan, Republic of China

[∥]Department of Biotechnology, National Formosa University, Yunlin 63208, Taiwan, Republic of China

[⊥]Graduate Institute of Biotechnology, National Chung Hsing University, Taichung 40227, Taiwan, Republic of China

Supporting Information

ABSTRACT: L-Amino acid oxidases (L-AAOs) have been isolated from many organisms, such as snake, and are known to have antibacterial activity. To the best of the authors' knowledge, this is the first report of the cloning of cDNA encoding a novel *Trichoderma harzianum* ETS 323 L-amino acid oxidase (Th-L-AAO). The protein was overexpressed in *Escherichia coli* and purified to homogeneity. Comparisons of its deduced amino acid sequence with the sequence of other L-AAOs revealed the similarity to be between 9 and 24%. The molecular mass of the purified protein was 52 kDa, as determined by sodium dodecyl sulfate−polyacrylamide gel electrophoresis. The enzyme substrate specificity was highest for L-phenylalanine, and its optimal pH and temperature for activity were 7 and 40 °C, respectively; exogenous metal ions had no significant effect on activity. Circular dichroism spectroscopy indicated that the secondary structure of Th-L-AAO is composed of 17% α-helices, 28% β-sheets, and 55% random coils. The bacterially expressed Th-L-AAO also mediated antibacterial activity against both Gram-positive and Gram-negative food spoilage microorganisms. Furthermore, a three-dimensional protein structure was created to provide more information about the structural composition of Th-L-AAO, suggesting that the N-terminal sequence of Th-L-AAO may have contributed to the antibacterial activity of this protein.

KEYWORDS: L-amino acid oxidase, L-phenylalanine oxidase, antibacterial, *Trichoderma harzianum*, *Escherichia coli*, *Staphylococcus aureus*

INTRODUCTION

Over the past few decades, many antibiotic proteins such as L-amino acid oxidases (L-AAOs) have been identified and isolated from organisms. L-AAOs have been studied since their discovery in the 1930s and have been identified in snake and insect venom,[1,2] fungi,[3] bacteria,[4] and algae.[5] L-AAOs are flavoproteins,[6] FAD-binding glycoproteins that catalyze the stereospecific oxidative deamination of L-amino acid substrates, producing the corresponding α-keto acids, ammonia, and hydrogen peroxide. These enzymes mediate antitumor effects[7] and induction of apoptosis,[8] as well as antibacterial[9] effects.

Some strains of *Escherichia coli* and *Staphylococcus aureus* can produce potentially lethal toxins. Food poisoning by *E. coli* is usually caused by the consumption of unwashed vegetables, undercooked meat, contaminated water, or unpasteurized milk. Certain strains of *S. aureus* are capable of producing heat-stable enterotoxins in food. In food-processing industries, chemical and biological residues inevitably accumulate on the surfaces of apparatuses in contact with food.[10] In fact, this microbial contamination possesses two components: the saprophytic flora responsible for food spoilage and the pathogenic flora that cause infections in humans and animals. Attachment of undesirable microorganisms to these surfaces is a concern because this can result in product contamination and, subsequently, serious agricultural, economic, and health-related problems.[11−13]

In our previous proteomic studies,[14] L-AAO was identified in *Trichoderma harzianum* ETS 323 grown in media containing a mixture of glucose with deactivated *Rhizoctonia solani* mycelia. During the subsequent study, the secretion of L-AAO by *T. harzianum* ETS 323 (Th-L-AAO) has been suggested to be associated with the antagonism of the plant pathogen *R. solani*.[15] However, no research has empirically investigated the biochemical properties and antibacterial activity of Th-L-AAO overexpressed by *E. coli*. Therefore, the goals of this study were to clone L-AAO cDNA from *T. harzianum* (GenBank accession no. GU902953), induce its expression in *E. coli*, purify it until homogeneity is achieved, and characterize the biochemical and antibacterial properties of this bacterially expressed protein.

Received: April 21, 2011
Revised: June 29, 2011
Accepted: July 28, 2011
Published: July 28, 2011

MATERIALS AND METHODS

Materials. All chemicals and the L-amino acid kit, *o*-dianisidine, and horseradish peroxidase (HRP) were purchased from Sigma-Aldrich (St. Louis, MO). Potato dextrose agar (PDA) was purchased from Difco (Becton, Dickinson and Co., Franklin Lakes, NJ), and dialysis membranes with a molecular weight cutoff of 12000−14000 were purchased from Spectrum (Rancho Dominguez, CA). The QIAEX Π Gel Extraction Kit was from Qiagen (Dusseldorf, Germany), and no. 1 filter paper was obtained from Advantec (Toyo Kaisha, Japan).

Media and Culture Conditions. *T. harzianum* ETS 323 (BCRC930081 accession number, Bioresource Collection and Research Center, Food Industry Research and Development Institute, Hsinchu, Taiwan) was grown on PDA plates at 25 °C for 7 days, after which 2 mL of sterile water was added to flush cells off the plate.[14] Conidia (about 10^6 mL^{-1}) were collected and used to inoculate 250 mL of minimal medium (pH 5.0), which contained 1.4 g L^{-1} $(NH_4)_2SO_4$, 2.0 g L^{-1} KH_2PO_4, 6.9 g L^{-1} NaH_2PO_4, 0.3 g L^{-1} $MgSO_4 \cdot 7H_2O$, 1.0 g L^{-1} peptone, 0.3 g L^{-1} urea, and 1% (w/v) glucose, in a 500 mL Erlenmeyer flask. Cultures were grown at 22 °C with shaking at 180 rpm for 7 days. The mycelia from the flask were then collected by filtration through cheesecloth and washed three times with sterile Milli-Q (18.2 MΩ) water and inoculated into fresh minimal medium containing 0.5% (w/v) glucose and 0.5% (w/v) deactivated *R. solani* mycelia. Cultures were grown for another 5 days at 22 °C with shaking at 180 rpm.[16] The culture media were removed by filtration using cheesecloth and then by no. 1 filter paper. RNA was prepared from the mycelia by grinding them with a mortar and pestle in liquid nitrogen. RNA was extracted using the TRIZOL reagent (Invitrogen, Carlsbad, CA) according to the manufacturer's instructions.

DNA Isolation and Manipulation. DNA isolation and manipulation were performed using a QIAEX II Gel Extraction Kit (Qiagen) as described previously.[17]

Amplification and Cloning of Th-L-AAO cDNA. By aligning *th-laao* coding sequences available in the NCBI database (GenBank accession no. AJ269533), specific primers (forward, 5′-TAG GCG CTG GTG TTT CCG-3′; reverse, 3′-ATC CGC GAC CAC AAA GGC-5′) were designed to amplify the *th-laao* cDNA. The pET29a vector (Novagen, Darmstadt, Germany) was used to clone the PCR products in which an *Nde*I site was introduced using the following modified primers: forward, 5′-CAT ATG GTA GGC GCT GGT GTT TCC G-3′; reverse, 5′-GTA TAC CAT CCG CGA CCA CAA AGG C-3′ (*Nde*I restriction sites are underlined). A partial *th-laao* gene (1589 bp) of *T. harzianum* ETS 323 was amplified using the primer and genomic DNA as the PCR template.

Reactions were performed in a Mastercycler Personal AG 22331 (Eppendorf, Hamburg, Germany). Amplification was performed at 94 °C for 5 min, followed by 28 cycles at 94 °C for 45 s, 55 °C for 45 s, and 72 °C for 1.5 min, and then 1 cycle at 72 °C for 10 min. The PCR product (1589 bp) was cloned into pET29a and verified by sequencing (Ming Hsin Biotechnology, Taipei, Taiwan).

Overexpression and Purification of Th-L-AAO. Recombinant plasmids were transformed into *E. coli* BL21 (DE3). A single transformed colony was selected and then grown at 37 °C overnight in 5 mL of Luria−Bertani (LB) medium containing kanamycin (50 μg mL^{-1}). The culture broth was diluted with this medium and incubated until the absorbance at 600 nm reached 0.6, and then 1 mM isopropyl-β-D-thiogalactopyranoside was added. After 4 h, cells were harvested by centrifugation for 10 min at 6000*g*, resuspended in 10 mM Tris-buffer (pH 8.3), and disrupted in sonication buffer (50 mM Tris-HCl (pH 8.0), 150 mM NaCl, 0.1% Tween 20, 1 mM phenylmethanesulfonyl fluoride (PMSF), and 10% glycerol (v/v)) using an ultrasonic generator (Microson XL2000 Ultrasonic Processor; Misonix, Farmingdale, NY).[18] The inclusion bodies of proteins were collected by centrifugation at 12000*g* for 15 min, and the pellets were dissolved in urea. Then, the protein-containing sample was dialyzed against ice-cold Milli-Q (18.2 MΩ) water in a dialysis membrane bag (molecular weight cutoff = 12000−14000) for 20 h at 4 °C, and the water was changed every 2 h. The His_6-tagged proteins were purified using a HisTrap affinity column (GE Healthcare, Uppsala, Sweden). The proteins were applied to the column in binding buffer (20 mM sodium phosphate, 0.5 M NaCl, and 17.5 mM imidazole (pH 7.4)) and eluted with 500 mM imidazole elution buffer. The resulting protein was desalted and concentrated with an Amicon ultracentrifugation device (30 kDa cutoff) and subjected to SDS-PAGE analysis.

Gel Electrophoresis. Enzyme purity and molecular weight were determined using 10% (w/v) sodium dodecyl sulfate−polyacrylamide gel electrophoresis (SDS-PAGE) (Protean II; Bio-Rad, Hercules, CA) following Laemmli's procedure.[19] Proteins were visualized by staining with colloidal Coomassie Blue G250 solution.[20]

L-AAO Activity Assay. An enzyme-coupled assay[21,22] was used to determine Th-L-AAO activity.[23,24] Briefly, hydrogen peroxide generated by Th-L-AAO in the presence of a certain test L-amino acid was treated with HRP and *o*-dianisidine. The 200 μL assay mixture contained 6 μL of HRP in 10 mM sodium phosphate buffer (pH 7.5), 20 μL of 5 mg mL^{-1} *o*-dianisidine dissolved in 20% Triton X-100, 0.1 M L-amino acid solution, and Th-L-AAO at 6 μM in 20 mM sodium phosphate buffer (pH 7.5). After 24 h at 37 °C, absorbance at A_{450} was determined using a plate reader (model 680; Bio-Rad).

Enzyme Characterization. To determine the optimal pH for 6 μM Th-L-AAO, different assay buffers were employed: 10 mM Tris-HCl (pH 8, 8.5, 9, 9.5, and 10), 10 mM phosphate (pH 6, 6.5, 7, and 7.5), and acetic acid (pH 3.5, 4, 4.5, 5, and 5.5).[25] Minor response variations of the *o*-dianisidine−peroxidase detection system for these buffers were adjusted by measuring standard curves at each pH with known amounts of H_2O_2. The optimal temperature for 6 μM Th-L-AAO was determined by assaying at 20, 30, 40, 50, 60, 70, 80, and 90 °C over 24 h. The effects of different metal ions and agents on enzyme activity were also determined. Twenty millimoles (in sterile Milli-Q (18.2 MΩ) water) of each metal ion (as $CaCl_2$, $MnCl_2$, $MgCl_2$, $HgCl_2$, $CoCl_2$, $CuCl_2$, $BaCl_2$, or KCl) was added to reaction mixtures (final ion concentration = 1 mM) and incubated at 37 °C for 24 h.

Kinetic Calculations. K_m and V_{max} were determined from a Lineweaver−Burk plot of data acquired by incubating 6 μM purified Th-L-AAO in 20 mM sodium phosphate buffer (pH 7.5) at 37 °C for 24 h. Plots were generated using Prism software (Origin 6.0; OriginLab, Northampton, MA).

Sequence Accession Number of *th-laao*. The nucleotide and protein sequences of *th-laao* were submitted to NCBI (GenBank accession no. GU902953).

Circular Dichroism (CD) Spectroscopy. The CD spectrum of Th-L-AAO (15.7 μg mL^{-1}) in 20 mM phosphate buffer (pH 7.5) was recorded using a J-715 CD spectropolarimeter (Jasco, Easton, MD). CD analysis was performed using a quartz optical cell with a 1 mm path length at 25 °C under continuous nitrogen flow. Each spectrum represents the mean of three measurements over 190−260 nm at 0.2 nm increments. The secondary structure was determined using the Dichroweb software (http://dichroweb.cryst.bbk.ac.uk/html/home.shtml).

Protein Modeling. Structural modeling was carried out using the Robetta server (http://robetta.bakerlab.org/) to create a three-dimensional (3D) protein structure based on the known X-ray structure of L-AAO of *Calloselasma rhodostoma* (PDB 2IID A). The Th-L-AAO structural model was generated by MolScript (http://www.avatar.se/molscript/) and Raster3D version 3.0 (http://skuld.bmsc.washington.edu/raster3d/raster3d.html), using the selected template.

Helical Wheel Analysis. The helical wheel was generated using the Pepwheel by EMBOSS explorer. The applet is accessible at http://emboss.bioinformatics.nl/cgi-bin/emboss/pepwheel.

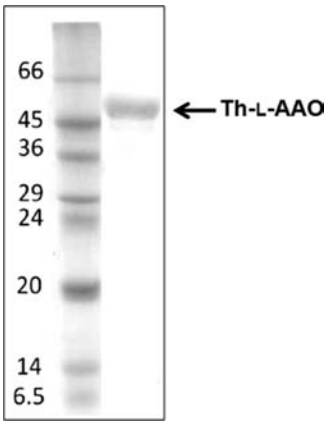

Figure 1. Purified Th-L-AAO from *T. harzianum* ETS 323 analyzed by 10% SDS-PAGE. Molecular mass standards: BSA, 66 kDa; ovalbumin, 45 kDa; glyceraldehyde-3-phosphate dehydryogenase, 36 kDa; carbonic anhydrase, 29 kDa; trypsinogen, 24 kDa; trypsin inhibitor, 20 kDa; α-lactalbumin, 14 kDa; aprotinin, 6.5 kDa.

Table 1. Kinetic Data of Th-L-AAO for 17 Different L-Amino Acid Substrates[a]

L-amino acid	V_{max} (μM)	K_m (mM)	k_{cat} (h^{-1})	k_{cat}/K_m ($mM^{-1}\ h^{-1}$)
L-Phe (F)	0.45	0.6	0.075	0.125
L-His (H)	0.64	1.77	0.11	0.062

[a] Th-L-AAO was ineffective with L-Gly, L-Leu, L-Val, L-Arg, L-Pro, L-Met, L-Lys, L-Glu, L-Gln, L-Ala, L-Thr, L-Ser, L-Asn, L-Trp, and L-Iso.

Antibacterial Activity of Th-L-AAO Produced in Bacterial Cells. *E. coli* (BCRC10675) and *S. aureus* (BCRC10780) were grown in LB medium for 24 h at 37 °C, and the medium was shaken at 150 rpm. Th-L-AAO (6 μM) was spotted onto LA plates that were streaked with 1×10^7 CFU mL^{-1} *S. aureus* or *E. coli*, and sterile water was added to the control. Following overnight incubation, the antibacterial effect was evidenced by a clear zone in the bacterial lawn.[26]

RESULTS

Expression and Purification of Th-L-AAO. To obtain Th-L-AAO for biochemical and antibacterial analyses, we overproduced Th-L-AAO in *E. coli* by using an expression vector (pET29a) containing *th-laao*. The resulting plasmid was transformed into *E. coli* BL21 (DE3). The Th-L-AAO from the inclusion body of crude *E. coli* BL21 (DE3) cell lysate was dissolved in urea, refolded by dialysis, and subsequently purified to homogeneity by using a HisTrap affinity column to obtain a yield of 112 mg L^{-1}. The apparent molecular mass of the purified protein was 52 kDa, as determined by SDS-PAGE (Figure 1).

Sequencing Analysis of *th-laao* and Comparison with Other L-AAOs. The verified nucleotide sequence of full-length *th-laao* cDNA (1589 bp) was submitted to GenBank and is assigned accession no. GU902953. The open reading frame comprised 1428 bp, encoding a protein comprising 476 amino acid residues from the initiating Met terminal residue, with a calculated molecular mass of 52.89 kDa. Sequence comparisons of Th-L-AAO with other L-AAO sequences using ClustalW2 (http://www.ebi.ac.uk/Tools/clustalw2/) revealed that there was limited similarity between Th-L-AAO and other L-AAO members, such as those from the fungi *Neurospora crassa* (24%) and *Aspergillus oryzae* (18%), the snakes *Pseudechis australis* (20%) and *Ophiophagus hannah* (20%), and the bacterium *Synechococcus elongatus* (9%) (Supporting Information, Figure S1). However, the amino acid sequence at the N-terminus of Th-L-AAO was identical among all sequences, demonstrating the presence of two highly conserved regions, a dinucleotide-binding domain and GG motifs.

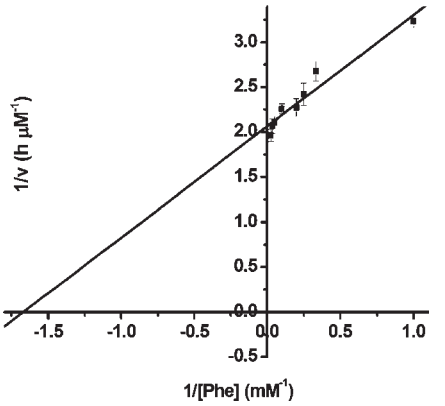

Figure 2. cDNA encoded Th-L-AAO K_m values for L-phenylalanine. Error bars represent the standard error, $n = 3$.

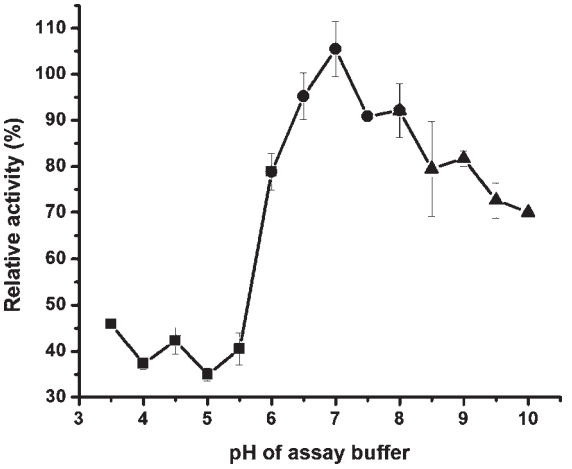

Figure 3. Effect of pH on cDNA-encoded Th-L-AAO activity. Enzyme activity was measured using L-phenylalanine. The square represents pH 3.5−5.5 (acetic acid buffer); the circle represents pH 6−7.5 (phosphate buffer); the triangle represents pH 8−10 (Tris-HCl). Error bars represent standard error, $n = 3$.

Substrate Specificity. The substrate specificity of cDNA-encoded Th-L-AAO was individually assayed with 17 L-amino acids. As shown in Table 1, Th-L-AAO showed detectable activity on phenylalanine and histidine. The kinetic parameters of these two amino acids, as determined by the Lineweaver−Burk plot, were $K_m = 0.6$ mM and $V_{max} = 0.45\ \mu M\ h^{-1}$ and $K_m = 1.77$ mM and $V_{max} = 0.64\ \mu M\ h^{-1}$ for phenylalanine (Figure 2) and histidine, respectively. The specific constants (k_{cat}/K_m) were 0.125 and 0.062 $mM^{-1}\ h^{-1}$ for phenylalanine and histidine, respectively (Table 1). However, Th-L-AAO did not show detectable activities to other amino acids. These results indicated that Th-L-AAO has the highest specificity for phenylalanine.

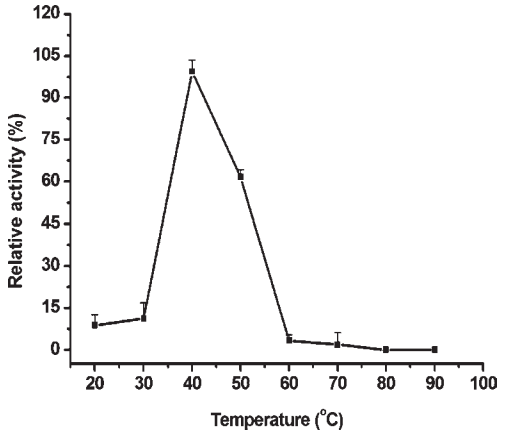

Figure 4. Effect of temperature on cDNA-encoded Th-L-AAO activity. Error bars represent the standard error, $n = 3$.

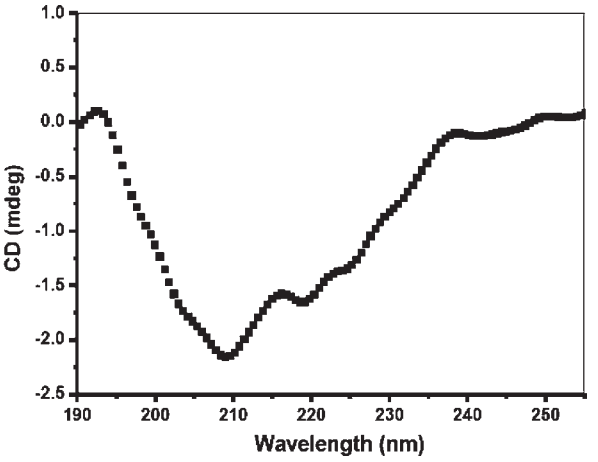

Figure 5. CD spectrum of cDNA-encoded Th-L-AAO.

Table 2. Effect of Ions on Th-L-AAO Activity

ion reagent[a]	relative activity (%)	ion reagent[a]	relative activity (%)
none	100	$MgCl_2$	100.4
$CaCl_2$	96.7	$HgCl_2$	99.7
$MnCl_2$	109.5	$CoCl_2$	101.1
$BaCl_2$	101.1	$CuCl_2$	103.8
KCl	99.9		

[a] The concentration of each ion reagent was 1 mM.

Optimum pH. The optimal pH of cDNA-encoded Th-L-AAO was determined, and L-phenylalanine was used as a substrate. The relative enzyme activity of cDNA-encoded Th-L-AAO was determined between pH 3.5 and 10. As shown in Figure 3, the activity of cDNA-encoded Th-L-AAO significantly decreased in the pH range 3.5−5.5 and >8, at which values 40−45 and 70−90% of the maximum activity, respectively, were retained. However, optimal activity to L-phenylalanine was observed between pH 6.5 and 8, with the maximum activity at pH 7 (Figure 3).

Optimum Temperature. The effect of temperature on the activity of cDNA-encoded Th-L-AAO was determined between 20 and 90 °C in 20 mM phosphate buffer (pH 7.5). L-Phenylalanine was used as a substrate. The results indicated that cDNA-encoded Th-L-AAO showed optimal activity at 40 °C (Figure 4). A strong decrease in activity was detected over ranges of 20−30 and 60−90 °C, compared to the activity at 40 °C. Moreover, 10 and 0% of maximum activities were retained at temperatures of 30 and >60 °C, respectively.

Effect of Metal Ions on cDNA Encoded Th-L-AAO Activity. Using L-phenylalanine as a substrate, the effect of various metal ions on the activity of cDNA-encoded Th-L-AAO was determined under optimal pH and temperature conditions (Table 2). The eight metal ions tested, Cu^{2+}, Ca^{2+}, Co^{2+}, Mn^{2+}, Mg^{2+}, Hg^{2+}, Ba^{2+}, and KCl, did not significantly affect hydrolysis, although a slight increase in activity was observed in the presence of $MnCl_2$ and $CuCl_2$.

Secondary Structural Contents of cDNA-Encoded Th-L-AAO. The secondary structural contents of this cDNA-encoded Th-L-AAO were determined by CD spectrometry in 20 mM sodium phosphate buffer (pH 7.5) (Figure 5) and calculated using Dichroweb software (http://dichroweb.cryst.bbk.ac.uk/html/home.shtml). The results indicated the composition of the secondary structures as 17% α-helices, 28% β-sheets, and 55% random coils.

3D Structural Simulation of Th-L-AAO. The 3D structure modeling of Th-L-AAO was conducted by the ROBETTA server as described under Materials and Methods. The overall structure of Th-L-AAO is shown in Figure 6. Th-L-AAO is a helix-rich protein, consisting of eight discontinuous regions of helical structure: residues 5−20, 64−73, 115−203, 219−230, 277−300, 385−398, 436−445, and 468−473 (Supporting Information, Figure S2). However, the simulated 3D structure of Th-L-AAO comprises 34% α-helices, 20% β-strands, and 46% random coils. Additionally, the FAD-binding site included a dinucleotide-binding domain (residues Gly3−Ala11) and GG motifs (residues Arg33−Thr40), which were indicated at the N-terminus of this protein (Figure 6A).

The N-linked glycosylation of native Th-L-AAO derived from *T. harzianum* ETS has been demonstrated in our previous study.[15] In this study, therefore, the possible glycosylation site of Th-L-AAO on the 3D protein structure was predicted by NetNGlyc 1.0 Server (http://www.cbs.dtu.dk/services/NetNGlyc/). Each N-linked glycosylation site at Asn (N) is shown in Figure 6B. The results indicated that Th-L-AAO has five glycosylation sites, at N22, N111, N206, N254, and N304 (Figure 6B; Supporting Information, Figure S3).

Antibacterial Activity of cDNA-Encoded Th-L-AAO against *E. coli* and *S. aureus*. Inhibition of the food spoilage bacteria *E. coli* and *S. aureus* by Th-L-AAO was tested in solid medium (Figure 7). Th-L-AAO-treated *E. coli* (Figure 7) showed an inhibition zone that was consistent with the results for kanamycin, a positive control. These results indicated that the cDNA-encoded Th-L-AAO has antibacterial activity, like the other L-AAO family members.[26,31,38]

DISCUSSION

To the best of our knowledge, this is the first report of bacterial expression of L-AAO derived from the fungus *T. harzianum* ETS 323, which has the best substrate specificity for phenylalanine. The molecular mass of this cDNA-encoded Th-L-AAO is 52 kDa, which is similar to the size of other deglycosylated L-AAOs, such as venom L-AAO RebO (51.9 kDa),[4] apoxin I (55 kDa),[23] and *Ophiophagus hannah* snake venom (53.68 kDa),[27] and that found in mouse milk (58 kDa).[26] In addition, on the basis of the results

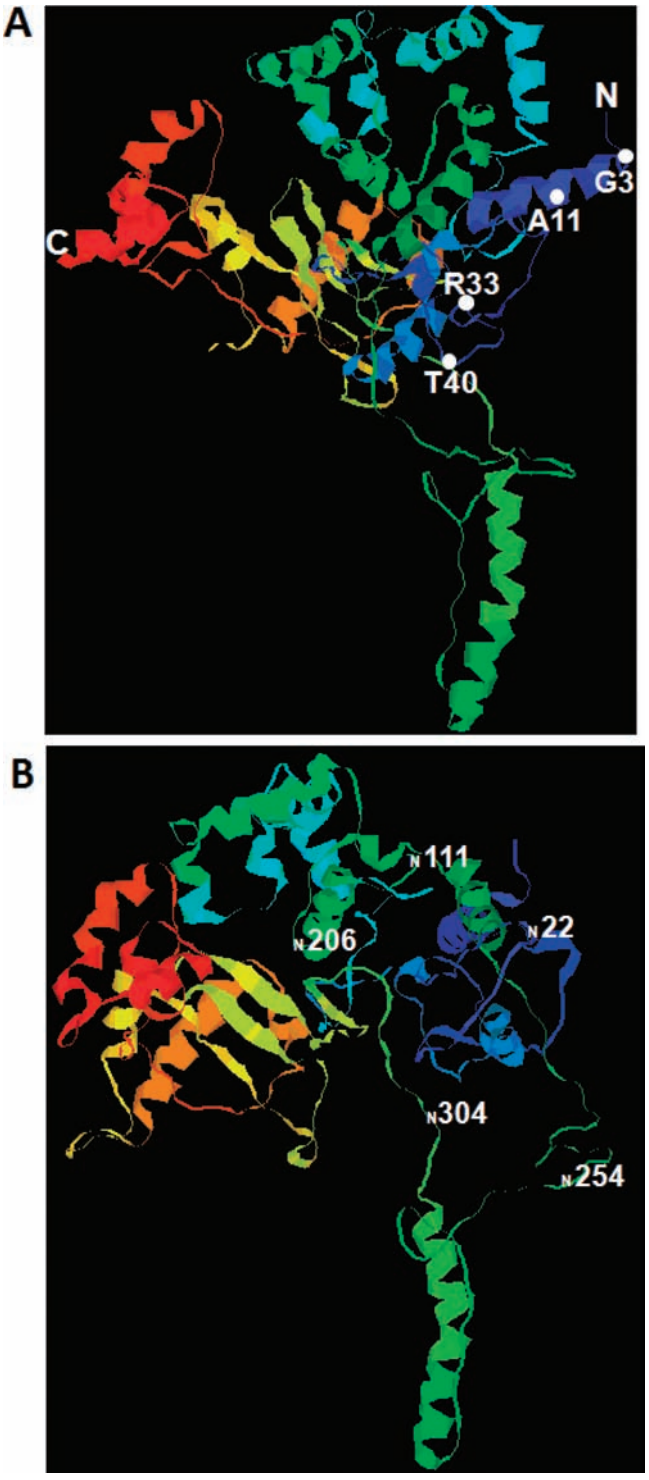

Figure 6. 3D protein structure and amphipathicity of Th-L-AAO. (A) Structural comparison of the overall structures of Th-L-AAO: top view of Th-L-AAO with an FAD-binding site in the model; the N and C terminals are colored blue and red, respectively. The FAD-binding site is shown in the N-terminal region, as a white point. (B) Five possible glycosylation sites in the Th-L-AAO model shown as Asn (N) amino acid positions 22, 111, 206, 254, and 304.

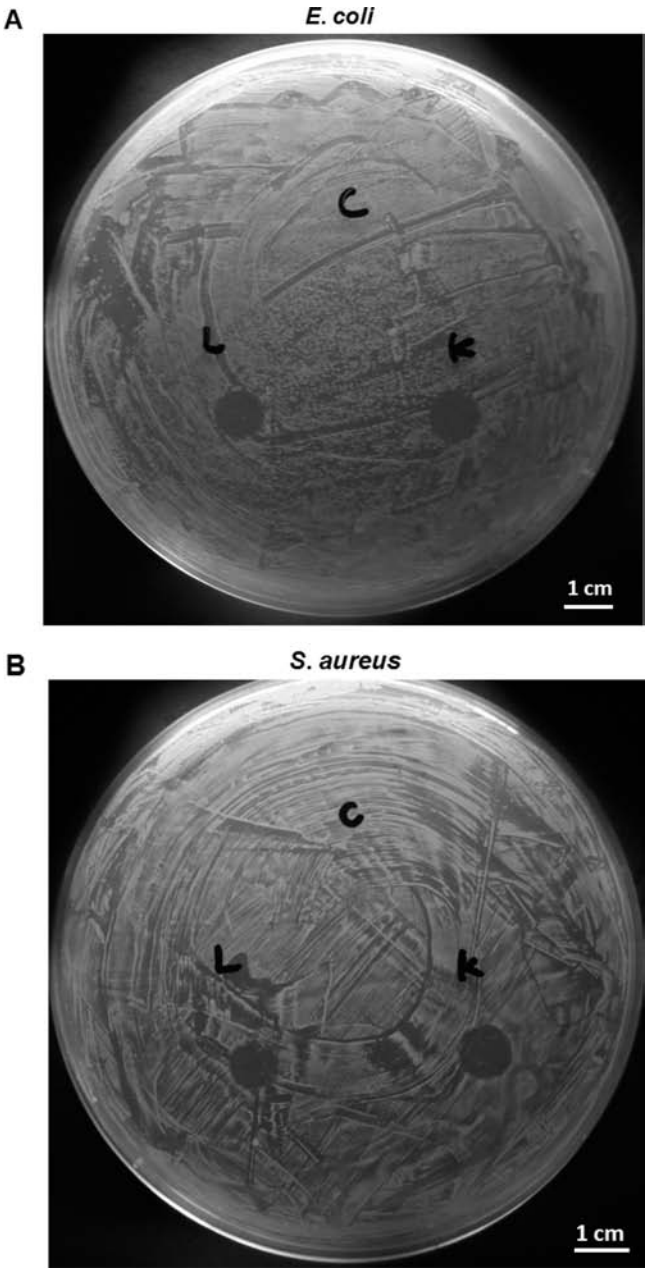

Figure 7. Antibacterial plate assay. Clear zones developed around the cDNA-encoded Th-L-AAO spots on plates seeded with (A) *E. coli* and (B) *S. aureus* for 24 h. C, negative control; L, 6 μM cDNA-encoded Th-L-AAO; K, 6 μM kanamycin.

of sequence alignment, the deduced amino acid sequence of Th-L-AAO has a low degree of similarity when compared with other L-AAOs; that is, Th-L-AAO is a novel L-AAO member, although Th-L-AAO contains two highly conserved motifs for FAD binding at the N-terminus, including the dinucleotide-binding domain and GG motif.

The optimal pH of this encoded Th-L-AAO is 7, which is identical with the optimal pH for the L-AAO of *Trichoderma viride* Y244-2.[3] The amino acid sequence of *T. viride* Y244-2 L-AAO was not reported, but Th-L-AAO and *T. viride* Y244-2 L-AAO contain an identical number of arginine (16 residues), cysteine (7 residues), methionine (11 residues), and proline (24 residues) residues, with little differences in the numbers of other amino acids, based on the analysis of acidic hydrolysis. Although they possess different substrate specificities, both L-AAOs share similar amino acid compositions and are from species belonging

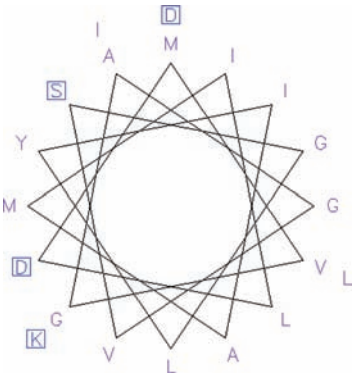

Figure 8. Helical wheel analysis of Th-L-AAO: graphical representation of the primary structures of Th-L-AAO, represented as two-dimensional axial projections, according to http://emboss.bioinformatics.nl/cgi-bin/emboss/pepwheel. It can be seen that the N-terminal sequence possesses a hydrophilic face composed of a polar and charged residues (square).

to the same genus. In contrast, most venom L-AAOs had an optimal pH value between 4 and 5[28−33] or between 8 and 9,[34] suggesting that these results may be due to the limited homology between Th-L-AAO and venom L-AAOs. Moreover, the optimal temperature for this protein was determined to be 40 °C. However, 10% of the maximum activity was retained at 30 °C, whereas the activity was 0% above 60 °C. One explanation is that, within limits, the rates of catalytic reaction increase with an increase in temperature, but thermal denaturation may occur at temperatures above 60 °C for Th-L-AAO.

The 3D simulated protein structure indicated that Th-L-AAO is a helix-rich protein and comprises 34% α-helices, 20% β-strands, and 46% random coils (Supporting Information, Figure S2). A similar secondary structure composition was shown in the native Th-L-AAO derived from *T. harzianum* ETS 323, 35% α-helices, 17% β-sheets, and 48% random coils (data not shown), but the cDNA-encoded Th-L-AAO consisted of 17% α-helices, 28% β-sheets, and 55% random coils. The structural modeling of Th-L-AAO was based on the known X-ray structure of L-AAO from the snake *C. rhodostoma* (PDB 2IID A). Therefore, there may have been some drawbacks of using *E. coli* for recombinant expression, including lack of post-translation modifications of the recombinant proteins (e.g., glycosylation) and chaperon-mediated complete protein folding.

The recent increase in foodborne illnesses around the world is a major health concern, most frequently caused by *E. coli* and *S. aureus*.[35] In this study, the cDNA-encoded Th-L-AAO also mediated antibacterial activity against both Gram-positive and Gram-negative food spoilage organisms, similar to other L-AAO family members.[7,36−39] However, even though the cDNA-encoded Th-L-AAO was overexpressed in *E. coli*, this protein has antibacterial activity against food spoilage by *E. coli* (BCRC10675). This result may be explained by considering that recombinant expression of proteins in bacterial hosts often results in the formation of insoluble inclusion bodies and subsequent misfolding and biological inactivation of proteins. Moreover, considering the results of the drawbacks of protein expression in *E. coli* together, we suggested that the global secondary structure and glycosylation of Th-L-AAO were not directly correlated with the antibacterial activity of this protein. In other words, the composition of the primary structure of Th-L-AAO may have a better relationship with its antibacterial effect.

On the basis of previous papers,[40,41] many antimicrobial peptides or proteins (AMPs) kill bacteria by permeabilization of the bacterial membrane. The positive hydrophobic moment and amphipathic α-helix at the N- or C-terminal sequence are hallmarks of most AMPs, thus allowing these proteins to bind to and penetrate bacterial membranes.[42] In this study, a helical structure was observed at the N-terminus of the simulated structure of Th-L-AAO, and a positive mean hydrophobic moment $\langle \mu_H \rangle$ (residues 1−30) of 0.75 was determined using the methodology of Kyte.[43] In light of these observations, helical wheel analysis of Th-L-AAO was further performed using a fixed angle of 100°. As shown in Figure 8, a distinct amphipathic pattern was observed, in which N-terminal residues are clustered closely in the center of the hydrophilic and hydrophobic face. Therefore, on the basis of this finding, we suggested that the antibacterial effect of Th-L-AAO may give rise to the hydrophobicity and amphipathicity phenomenon at its N-terminus. It will be interesting to determine whether other L-AAOs have this antibacterial property. The preliminary results showed that a considerable number of cytotoxic L-AAOs have positive hydrophobic moment and amphipathicity at the N-terminus, similar to Th-L-AAO.

However, some previous studies have proposed that L-AAO-induced cytotoxic effects are via H_2O_2 production because the catalase[8] and ascorbic acid[44] can recover partial viability of L-AAO-treated cells. In light of this, the catalase (0.5 mg mL^{-1}) was applied directly to Th-L-AAO-treated bacteria, but no expected growth recovery was observed for either bacterial strain by antibacterial plate assay. These results suggested that the H_2O_2 production cannot fully explain the cytotoxic effect of L-AAO. In other words, the permeabilization of the bacterial membrane may be another essential mechanism of cytotoxic effect of L-AAO. More research along these lines is required, but we anticipate that these results will be beneficial to understanding the antibacterial effect of L-AAOs.

■ ASSOCIATED CONTENT

Ⓢ Supporting Information. Three additional figures. This material is available free of charge via the Internet at http://pubs.acs.org.

■ AUTHOR INFORMATION

Corresponding Author

*Phone: +886 3 8633635. Fax: +886 3 8633630. Postal address: No. 1, Sec. 2, Da Hsueh Rd., Shoufeng, Hualien 97401, Taiwan, ROC. E-mail: kcpeng@mail.ndhu.edu.tw.

Funding Sources

The work was supported by the NSC, Taiwan, under Grant NSC-99-2313-B-212-001-MY3.

■ REFERENCES

(1) Lukasheva, E. V.; Berezov, T. T. L-Lysine α oxidase: physicochemical and biological properties. *Biochemistry (Moscow)* **2002**, *67*, 1152–1158.

(2) Ahn, M. Y.; Lee, B. M.; Kim, Y. S. Characterization and cytotoxicity of L-amino acid oxidase from the venom of king cobra (*Ophiophagus hannah*). *Int. J. Biochem. Cell Biol.* **1997**, *29*, 911–919.

(3) Kusakabe, H.; Kodama, K.; Kuninaka, A.; Yoshino, H. A new antitumor enzyme, L-lysine α-oxidase from *Trichoderma viride*. *J. Biol. Chem.* **1980**, *255*, 976–981.

(4) Nishizawa, T.; Courtney, C. A.; David, H. S. Molecular analysis of the rebeccamycin L-amino acid oxidase from *Lechevalieria aerocolonigenes* ATCC 39243. *J. Bacteriol.* **2005**, *187*, 2084–2092.

(5) Vallon, O.; Bulté, L.; Olive, J.; Wollman, F. A. Extensive accumulation of an extracellular L-amino-acid oxidase during gametogenesis of *Chlumydomonas reinhardtii*. *Eur. J. Biochem.* **1993**, *215*, 351–360.

(6) Pawelek, P. D.; Cheah, J.; Coulombe, R.; Macheroux, P.; Ghisla, S.; Vrielink, A. The structure of L-amino acid oxidase reveals the substrate trajectory into an enantiomerically conserved active site. *EMBO J.* **2000**, *19*, 4204–4215.

(7) Rodrigues, R. S.; da Silva, J. F.; Boldrini França, J.; Fonseca, F. P.; Otaviano, A. R.; Henrique Silva, F.; Hamaguchi, A.; Magro, A. J.; Braz, A. S.; dos Santos, J. I.; Homsi-Brandeburgo, M. I.; Fontes, M. R.; Fuly, A. L.; Soares, A. M.; Rodrigues, V. M. Structural and functional properties of Bp-L-AAO, a new L-amino acid oxidase isolated from *Bothrops pauloensis* snake venom. *Biochimie* **2009**, *91*, 490–501.

(8) Torii, S.; Naito, M.; Tsuruo, T. Apoxin I, a novel apoptosis-inducing factor with L-amino acid oxidase activity purified from western diamondback rattlesnake venom. *J. Biol. Chem.* **1997**, *272*, 9539–9542.

(9) Ciscotto, P.; Machado de Avila, R. A.; Coelho, E. A.; Oliveira, J.; Diniz, C. G.; Farías, L. M.; de Carvalho, M. A.; Maria, W. S.; Sanchez, E. F.; Borges, A.; Chávez, O. C. Antigenic, microbicidal and antiparasitic properties of an L-amino acid oxidase isolated from *Bothrops jararaca* snake venom. *Toxicon* **2009**, *53*, 330–341.

(10) Loeb, G. I.; Neihof, R. A. Marine conditioning films. In *Applied Chemistry at Protein Interfaces,* ; Advances in Chemistry Series 145; American Chemical Society: Washington, DC, 1975; pp 319−335

(11) Carpentier, B.; Cerf, O. Biofilms and their consequences with particular reference to hygiene in the food industry. *J. Appl. Microbiol.* **1993**, 499−511.

(12) McFeters, G. A.; Bazin, M. J.; Bryers, J. D. In *Biofilm Development and Its Consequences in Microbial Adhesion and Aggregation*; Marshall, K. C., Ed.; Springer: Berlin, Germany, 1984; pp 109−124.

(13) Mueller, R. F. Bacterial transport and colonization in low nutrient environments. *Water Res.* **1996**, *30*, 2681–2690.

(14) Tseng, S. C.; Liu, S. Y.; Yang, H. H.; Lo, C. T.; Peng, K. C. Proteomic study of biocontrol mechanisms of *Trichoderma harzianum* ETS 323 in response to *Rhizoctonia solani*. *J. Agric. Food Chem.* **2008**, *56*, 6914–6922.

(15) Yang, C. A.; Cheng, C. H.; Lo, C. T.; Liu, S. Y.; Lee, J. W.; Peng, K. C. A novel L-amino acid oxidase from *Trichoderma harzianum* ETS 323 associated with antagonism of *Rhizoctonia solani*. *J. Agric. Food Chem.* **2011**, *59*, 4519−4526.

(16) Liu, S. Y.; Chen, C.; Liu, M. Y.; Chen, J. H.; Peng, K. C. Efficient isolation of anthraquinone-derivatives from *Trichoderma harzianum* ETS 323. *J. Biochem. Biophys. Methods* **2007**, *70*, 391–395.

(17) Sambrook, J.; Russel, D. W. *Molecular Cloning: A Laboratory Manual*, 3rd ed.; Cold Spring Harbor Laboratory Press: Cold Spring Harbor, NY, 2000.

(18) Miki, Y.; Morales, M.; Ruiz-Dueñas, F. J.; Martínez, M. J.; Wariishi, H.; Martínez, A. T. *Escherichia coli* expression and in vitro activation of a unique ligninolytic peroxidase that has a catalytic tyrosine residue. *Protein Expr. Purif.* **2009**, *68*, 208–214.

(19) Laemmli, U. K. Cleavage of structural proteins during the assembly of the head of bacteriophage T4. *Nature* **1970**, *227*, 680–685.

(20) Neuhoff, V.; Arold, N.; Taube, D.; Ehrhardt, W. Improved staining of proteins in polyacrylamide gels including isoelectric focusing gels with clear background at nanogram sensitivity using Coomassie Brilliant Blue G-250 and R-250. *Electrophoresis* **1988**, *9*, 255–262.

(21) Avrameas, S.; Guilbart, B. Enzyme-immunoassay for the measurement of antigens using peroxidase conjugates. *Biochimie* **1972**, *54*, 837–842.

(22) Geueke, B.; Hummel, W. A new bacterial L-amino acid oxidase with a broad substrate specificity: purification and characterization. *Enzyme Microb. Technol.* **2002**, *31*, 77–87.

(23) Torii, S.; Tsuruo, T. Molecular cloning and functional analysis of apoxin I, a snake venom-derived apoptosis-inducing factor with L-amino acid oxidase activity. *Biochemistry* **2000**, *39*, 3197–3205.

(24) Kommoju, P. R.; Ghisla, S. Molecular cloning, expression and purification of L-amino acid oxidase from the Malayan pit viper *Calloselasma rhodostoma*. *Protein Expr. Purif.* **2007**, *52*, 89–95.

(25) Ellis, K. J.; Morrison, J. F. Buffers of constant ionic strength for studying pH-dependent processes. *Methods Enzymol.* **1982**, *87*, 405–426.

(26) Nagaoka, K.; Aoki, F.; Hayashi, M.; Muroi, Y.; Sakurai, T.; Toh, I. K.; Ikawa, M.; Imakawa, K.; Sakai, S. L-amino acid oxidase plays a crucial role in host defense in the mammary glands. *FASEB J.* **2009**, *23*, 2514–2520.

(27) Jin, Y.; Lee, W. H.; Zeng, L.; Zhang, Y. Molecular characterization of L-amino acid oxidase from king cobra venom. *Toxicon* **2007**, *50*, 479–89.

(28) Sun, M. Z.; Guo, C.; Tian, Y.; Chen, D.; Greenaway, F. T.; Liu, S. Biochemical, functional and structural characterization of Akbu-LAAO: a novel snake venom L-amino acid oxidase from *Agkistrodon blomhoffii ussurensis*. *Biochimie* **2010**, *92*, 343–349.

(29) Ponnudurai, G.; Chung, M. C.; Tan, N. H. Purification and properties of the L-amino acid oxidase from Malayan pit viper (*Calloselasma rhodostoma*) venom. *Arch. Biochem. Biophys.* **1994**, *313*, 373–378.

(30) Ueda, M.; Chang, C. C.; Ohno, M. Purification and characterization of L-amino acid oxidase fromthe venomof *Trimeresurus mucrosquamatus* (Taiwan habu snake). *Toxicon* **1988**, *26*, 695–706.

(31) Wellner, D.; Meister, A. Crystalline L-amino acid oxidase of *Crotalus adamanteus*. *J. Biol. Chem.* **1960**, *235*, 2013–2018.

(32) Li, Z. Y.; Yu, T. F.; Lian, E. C. Purification and characterization of L-amino acid oxidase from king cobra (*Ophiophagus hannah*) venom and its effects on human platelet aggregation. *Toxicon* **1994**, *32*, 1349–1358.

(33) Wei, X. L.; Wei, J. F.; Li, T.; Qiao, L. Y.; Liu, Y. L.; Huang, T.; He, S. H. Purification, characterization and potent lung lesion activity of an L-amino acid oxidase from *Agkistrodon blomhoffii ussurensis* snake venom. *Toxicon* **2007**, *50*, 1126–1139.

(34) Nuutinen, J. T.; Timonen, S. Identification of nitrogen mineralization enzymes, L-amino acid oxidases, from the ectomycorrhizal fungi *Hebeloma* spp. and *Laccaria bicolor*. *Mycol. Res.* **2008**, *112*, 1453–1464.

(35) Flores, V. H.; Canizalez, R. A.; Reyes, L. M.; Nazmi, K.; de la Garza, M.; Zazueta, B. J.; León, S. N.; Bolscher, J. G. Bactericidal effect of bovine lactoferrin, LFcin, LFampin and LFchimera on antibiotic-resistant *Staphylococcus aureus* and *Escherichia coli*. *Biometals* **2010**, *23*, 569–578.

(36) Tõnismägi, K.; Samel, M.; Trummal, K.; Rönnholm, G.; Siigur, J.; Kalkkinen, N.; Siigur, E. L-Amino acid oxidase from *Vipera lebetina* venom: isolation, characterization, effects on platelets and bacteria. *Toxicon* **2006**, *48*, 227–237.

(37) Samel, M.; Tõnismägi, K.; Rönnholm, G.; Vija, H.; Siigur, J.; Kalkkinen, N.; Siigur, E. L-Amino acid oxidase from *Naja naja oxiana* venom. *Comp. Biochem. Physiol. B: Biochem. Mol. Biol.* **2008**, *149*, 572–580.

(38) Zhong, S. R.; Jin, Y.; Wu, J. B.; Jia, Y. H.; Xu, G. L.; Wang, G. C.; Xiong, Y. L.; Lu, Q. M. Purification and characterization of a new L-amino acid oxidase from *Daboia russellii siamensis* venom. *Toxicon* **2009**, *54*, 763–771.

(39) Kitani, Y.; Ishida, M.; Ishizaki, S.; Nagashima, Y. Discovery of serum L-amino acid oxidase in the rockfish *Sebastes schlegeli*: isolation and biochemical characterization. *Comp. Biochem. Physiol. B: Biochem. Mol. Biol.* **2010**, *157*, 351–356.

(40) Toke, O. Antimicrobial peptides: new candidates in the fight against bacterial infections. *Biopolymers* **2005**, *80*, 717–35.

(41) Jenssen, H.; Hamill, P.; Hancock, R. E. Peptide antimicrobial agents. *Clin. Microbiol. Rev.* **2006**, *19*, 491–511.

(42) Chongsiriwatana, N. P.; Patch, J. A.; Czyzewski, A. M.; Dohm, M. T.; Ivankin, A.; Gidalevitz, D.; Zuckermann, R. N.; Barron, A. E. Peptoids that mimic the structure, function, and mechanism of helical antimicrobial peptides. *Proc. Natl. Acad. Sci.U.S.A.* **2008**, *105*, 2794–2799.

(43) Kyte, J.; Doolittle, R. F. A simple method for displaying the hydropathic character of a protein. *J. Mol. Biol.* **1982**, *157*, 105–132.

(44) Stasyk, T.; Lutsik-Kordovsky, M.; Wernstedt, C.; Antonyuk, V.; Klyuchivska, O.; Souchelnytskyi, S.; Hellman, U.; Stoika, R A new highly toxic protein isolated from the death cap *Amanita phalloides* is an L-amino acid oxidase. *FEBS J.* **2010**, *277*, 1260–1269.